

Evidence for Inflation in an Axion Landscape

Pran Nath and Maksim Piskunov

*Department of Physics, Northeastern University,
Boston, MA 02115-5000, USA*

E-mail: p.nath@northeastern.edu, m.piskunov@northeastern.edu

ABSTRACT: We discuss inflation models within supersymmetry and supergravity frameworks with a landscape of chiral superfields and one $U(1)$ shift symmetry which is broken by non-perturbative symmetry breaking terms in the superpotential. We label the pseudo scalar component of the chiral fields axions and their real parts saxions. Thus in the models only one combination of axions will be a pseudo-Nambu-Goldstone-boson which will act as the inflaton. The proposed models constitute consistent inflation for the following reasons: The inflation potential arises dynamically with stabilized saxions, the axion decay constant can lie in the sub-Planckian region, and consistency with the Planck data is achieved. The axion landscape consisting of m axion pairs is assumed with the axions in each pair having opposite charges. A fast roll–slow roll splitting mechanism for the axion potential is proposed which is realized with a special choice of the axion basis. In this basis the $2m$ coupled equations split into $2m - 1$ equations which enter in the fast roll and there is one unique linear combination of the $2m$ fields which controls the slow roll and thus the power spectrum of curvature and tensor perturbations. It is shown that a significant part of the parameter space exists where inflation is successful, i.e., $N_{\text{pivot}} = [50, 60]$, the spectral index n_s of curvature perturbations, and the ratio r of the power spectrum of tensor perturbations and curvature perturbations, lie in the experimentally allowed regions given by the Planck experiment. Further, it is shown that the model allows for a significant region of the parameter space where the effective axion decay constant can lie in the sub-Planckian domain. An analysis of the tensor spectral index n_t is also given and the future experimental data which constraints n_t will further narrow down the parameter space of the proposed inflationary models. Topics of further interest include implications of the model for gravitational waves and non-Gaussianities in the curvature perturbations. Also of interest is embedding of the model in strings which are expected to possess a large axionic landscape.

Contents

1	Introduction	1
2	A supersymmetric model of inflation for an axionic landscape	3
3	The axion landscape and a Fast roll-Slow roll splitting mechanism	6
4	Extension to supergravity	8
5	Consistency with Planck data [10, 11]	10
5.1	Experimental observables	10
5.2	Monte Carlo Analysis for fit to data	11
5.3	Generation of a flat inflation potential	14
6	Conclusion	15
7	Appendix A: Preliminaries	16
8	Appendix B: Power spectrum and Spectral Indices	17
9	Appendix C: Emergence of a flat inflation potential for axions	19

1 Introduction

Inflationary models resolve a number of problems associated with Big Bang cosmology which include the flatness problem, the horizon problem, and the monopole problem [1–6] (for a review see [7] and for effective field theory of inflation see [8]). In inflation models quantum fluctuations at the time of horizon exit carry significant information regarding the characteristics of the inflationary model [9]. The cosmic microwave background (CMB) radiation anisotropy allows extraction of such characteristics which can discriminate among models. Thus recently the astrophysical data from the Planck experiment [10–12] has put significant constraints on models eliminating many and reducing the parameter space of others. One class of models are those associated with the so called natural inflation where the inflaton is an axionic field. Thus natural inflation is described by a simple potential [13, 14]

$$V(a) = \Lambda^4 \left(1 + \cos\left(\frac{a}{f}\right) \right), \quad (1.1)$$

where a is the axion field and f is the axion decay constant. The Planck data requires f significantly greater M_{Pl} , i.e., $f > 10M_{Pl}$ where M_{Pl} is the Planck mass. Now $f > M_{Pl}$

is undesirable since a global symmetry is not preserved by quantum gravity unless it has a gauge origin. Further, string theory prefers f below M_{PL} [15, 16]. Reduction of the axion decay constant turns out to be a significant problem and various procedures have been pursued to overcome it. These include the so called alignment mechanism [17, 18], the two axion Dante’s inferno model [19] and N-flation [20–28]. Other models using shift symmetry include [29–32] (for a review and a more extensive set of references of axionic inflation and of axionic cosmology see [33, 34].).

In this work we introduce an inflation model in an axion landscape with a $U(1)$ symmetry and with m pairs of chiral fields where the chiral fields in each pair are oppositely charged under the same $U(1)$ global symmetry. We wish to note here that different authors define the term “axion” differently. In the analysis here we will use the term “axion” for the pseudo-scalar component of any chiral field and the corresponding real part will be called a “saxion”. In our analysis we have only one $U(1)$ global symmetry and thus breaking of it would lead to only one pseudo-Nambu-Goldstone-boson (PNGB) and the remaining pseudo-scalars are not PNGBs. It is important to keep this distinction in mind since sometimes the term “axion” is automatically interpreted as being a PNGB which is not the case in the analysis here. Returning to the construction of our model the superpotential is chosen to consist of two parts where one part is invariant under the $U(1)$ symmetry and the other consists of a symmetry breaking piece such as the one arising from instanton effects. Here we show that a fast roll-slow roll splitting mechanism exists which allows a decomposition of the axion potential into a fast roll and a slow roll part where inflation is driven by the slow roll part. This set up reduces a multi-field coupled axion system with $2m$ axions to an effective single axion field potential which controls inflation. Using this set up we analyze both supersymmetry and supergravity models and show that under the constraints of stabilized saxions, one can find inflation models with the axion decay constant $f < M_{Pl}$ consistent with the data from the Planck experiment.

The outline of the rest of the paper is as follows. In section 2, we describe the supersymmetric model of inflation for an axionic landscape consisting of m pairs of axions with each pair oppositely charged under the $U(1)$ symmetry. The superpotential consists of two terms: a part which is invariant under the $U(1)$ symmetry and a part which breaks it arising possibly from instantons. Using this superpotential we deduce the conditions for stabilized saxions and then compute the scalar potential for the axions under the constraints of stabilized saxions. In this section we also compute the axion mass matrices. In section 3, we carry out a decomposition of the scalar axion potential into a fast roll and a slow part. To accomplish this we first find the basis where $2m - 1$ axions are heavy and one axion is light, i.e., massless in the limit when there is no breaking of the shift symmetry. Part of the potential which contains the heavy fields produces the fast roll inflation while the part that contains the light field generates the slow roll part. The decomposition reduces the multi-field inflation to a single field inflation. Here we also show that in the slow roll part an effective axion decay constant f_e enters which is given by $f_e = \sqrt{2m}f$ where f is the common decay constant of the axions that enter the superpotential. This result was first derived in [20] but here we give a more general derivation of it. In section 4, we extend

the analysis of section 3 to supergravity with similar conclusions. In section 5, we give an analysis of the number of e-foldings, of the power spectrum for curvature and tensor perturbations, and of the scalar and of the tensor spectral indices. Specifically we show that much of the allowed parameter space of experiment is accessible in this model and future experiment will constrain the model more stringently. In this section we also show how the cosine functions generate a locally flat potential necessary for inflation. Conclusions are given in section 6. In appendices A and B we define notation and give some mathematical background useful for the analysis carried out in section 5. In Appendix C we illustrate the emergence of a flat inflation potential arising from the superposition of cosine functions.

2 A supersymmetric model of inflation for an axionic landscape

We discuss here a general supersymmetric framework for axionic inflation to occur¹. The axions we consider are not QCD axions [43–45] which were originally the basis of the analysis of [13]. In string theory axions occur which are not related to the QCD axions [16, 46]. Thus we consider the existence of a shift symmetry and assume that in an axionic landscape, such as the one that one might expect in string theory, there are a number of axionic fields carrying the same $U(1)$ quantum number. Now suppose we have a set of fields S_i ($i = 1, \dots, m$) where S_i carry the same charge under the shift symmetry and the fields \bar{S}_i ($i = 1, \dots, m$) carry the opposite charge. Thus under $U(1)$ transformations one has

$$S_i \rightarrow e^{iq\lambda} S_i, \quad \bar{S}_i \rightarrow e^{-iq\lambda} \bar{S}_i, \quad i = 1, \dots, m. \quad (2.1)$$

The superfields S_i have an expansion,

$$S_i = \phi_i + \theta\chi_i + \theta\theta F_i, \quad (2.2)$$

where ϕ_i is a complex scalar field consisting of the saxion (the real part) and the axion (the imaginary part), χ_i is the axino, and F_i is an auxiliary field. Similarly the superfields \bar{S}_i have an expansion: $\bar{S}_i = \bar{\phi}_i + \bar{\theta}\bar{\chi}_i + \bar{\theta}\bar{\theta}\bar{F}_i$. We now consider a superpotential of the form

$$W = W_s(S, \bar{S}) + W_{sb}(S, \bar{S}), \quad (2.3)$$

where W_s is the part that depends on the fields S_i, \bar{S}_i and is invariant under the shift symmetry. W_{sb} is a part which breaks the shift symmetry and has the form

$$W_{sb} = \sum_i A_i(S, \bar{S}) e^{-T_i}, \quad (2.4)$$

where T_i is the action of the i -th instanton. In general gauge invariance and holomorphy allow non-perturbative terms of the type

$$A \frac{S^n}{M_P^{n-3}} e^{-T}, \quad \bar{A} \frac{\bar{S}^n}{M_P^{n-3}} e^{-T}. \quad (2.5)$$

¹For references to early work in supersymmetry and supergravity see [35–39, 41, 42, 66].

Detailed structure will depend on the instanton zero modes (see [46, 47] and the references there in). Thus we assume the following forms for $W(S, \bar{S})$ ²

$$W(S, \bar{S}) = \sum_{k=1}^m \sum_{l=1}^m \left(\mu_{kl} S_k \bar{S}_l + \frac{\lambda_{kl}}{2M} (S_k \bar{S}_l)^2 \right) + \sum_{k=1}^m \sum_{l=1}^q A_{kl} S_k^l + \sum_{k=1}^m \sum_{l=1}^q \bar{A}_{kl} \bar{S}_k^l. \quad (2.6)$$

Here the terms in the first brace on the right hand side are invariant under the shift symmetry while the remaining terms on the right hand side violate the shift symmetry. The variation of the superpotential with respect to ϕ_k and $\bar{\phi}_k$ generate the constraints that determine the VEVs of ϕ_k and $\bar{\phi}_k$. We assume CP conserving vacua so that the VEVs of the CP odd axionic fields vanish while we set $f_k = \langle \phi_k \rangle$ and $\bar{f}_k = \langle \bar{\phi}_k \rangle$. The constraint equations arising from the variation of the superpotential with respect to ϕ_k and $\bar{\phi}_k$ are

$$\begin{aligned} \frac{\partial W(\phi, \bar{\phi})}{\partial \phi_k} &= 0, \\ \frac{\partial W(\phi, \bar{\phi})}{\partial \bar{\phi}_k} &= 0. \end{aligned} \quad (2.7)$$

We may parametrize ϕ_k and $\bar{\phi}_k$ so that

$$\phi_k = (f_k + \rho_k) e^{ia_k/f_k}, \quad \bar{\phi}_k = (\bar{f}_k + \bar{\rho}_k) e^{i\bar{a}_k/\bar{f}_k}, \quad (2.8)$$

where $f_k = \langle \phi_k \rangle$, $\bar{f}_k = \langle \bar{\phi}_k \rangle$ and (ρ_k, a_k) and $(\bar{\rho}_k, \bar{a}_k)$ are the fluctuations of the quantum fields around their vacuum expectation values $f_k(\bar{f}_k)$. They are constrained by the stability conditions for the saxions Eqs. (2.7) which give

$$\begin{aligned} \sum_{l=1}^m \left(\mu_{kl} \bar{f}_l + \frac{\lambda_{kl}}{M} f_k \bar{f}_l^2 \right) + \sum_{l=1}^q l A_{kl} f_k^{l-1} &= 0, \\ \sum_{l=1}^m \left(\mu_{lk} f_l + \frac{\lambda_{lk}}{M} f_l^2 \bar{f}_k \right) + \sum_{l=1}^q l \bar{A}_{kl} \bar{f}_k^{l-1} &= 0. \end{aligned} \quad (2.9)$$

We focus here on the scalar potential for the axions and thus we expand around the minimum of the potential of the saxions, i.e., we set $\rho_k = 0 = \bar{\rho}_k$. Using the saxion stability

²A simplified version of this form of the superpotential has been considered recently in the context of an ultralight axion [46].

conditions given by Eq.(2.9) a somewhat lengthy computation gives for the scalar potential

$$V(a, \bar{a}) = V_s(a, \bar{a}) + V_{sb}(a, \bar{a}), \quad (2.10)$$

where

$$\begin{aligned} V_s(a, \bar{a}) = & \sum_{k=1}^m \left(\sum_{l=1}^m \sum_{p=1}^m (\mu_{kl} \mu_{kp} \bar{f}_l \bar{f}_p \cos \left(\frac{\bar{a}_p}{\bar{f}_p} - \frac{\bar{a}_l}{\bar{f}_l} \right) + \mu_{lk} \mu_{pk} f_l f_p \cos \left(\frac{a_p}{f_p} - \frac{a_l}{f_l} \right) \right. \\ & + \frac{\lambda_{kl}}{M} \frac{\lambda_{kp}}{M} f_k^2 \bar{f}_l^2 \bar{f}_p^2 \cos \left(2 \frac{\bar{a}_p}{\bar{f}_p} - 2 \frac{\bar{a}_l}{\bar{f}_l} \right) + \frac{\lambda_{lk}}{M} \frac{\lambda_{pk}}{M} f_l^2 f_p^2 \bar{f}_k^2 \cos \left(2 \frac{a_p}{f_p} - 2 \frac{a_l}{f_l} \right) \\ & \left. + 2 \mu_{kl} \frac{\lambda_{kp}}{M} f_k \bar{f}_l \bar{f}_p^2 \cos \left(\frac{a_k}{f_k} + 2 \frac{\bar{a}_p}{\bar{f}_p} - \frac{\bar{a}_l}{\bar{f}_l} \right) + 2 \mu_{lk} \frac{\lambda_{pk}}{M} \bar{f}_k f_l f_p^2 \cos \left(\frac{\bar{a}_k}{\bar{f}_k} + 2 \frac{a_p}{f_p} - \frac{a_l}{f_l} \right) \right), \quad (2.11) \end{aligned}$$

and

$$\begin{aligned} V_{sb}(a, \bar{a}) = & \sum_{l=1}^m \sum_{r=1}^q (2r A_{kr} \mu_{kl} f_k^{r-1} \bar{f}_l \cos \left((r-1) \frac{a_k}{f_k} - \frac{\bar{a}_l}{\bar{f}_l} \right) \\ & + 2r \bar{A}_{kr} \mu_{lk} \bar{f}_k^{r-1} f_l \cos \left((r-1) \frac{\bar{a}_k}{\bar{f}_k} - \frac{a_l}{f_l} \right) \\ & + 2r A_{kr} \frac{\lambda_{kl}}{M} f_k^r \bar{f}_l^2 \cos \left((r-2) \frac{a_k}{f_k} - 2 \frac{\bar{a}_l}{\bar{f}_l} \right) + 2r \bar{A}_{kr} \frac{\lambda_{lk}}{M} \bar{f}_k^r f_l^2 \cos \left((r-2) \frac{\bar{a}_k}{\bar{f}_k} - 2 \frac{a_l}{f_l} \right) \\ & + \sum_{l=1}^q \sum_{r=1}^q \left(l r A_{kl} A_{kr} f_k^{l+r-2} \cos \left((r-l) \frac{a_k}{f_k} \right) + l r \bar{A}_{kl} \bar{A}_{kr} \bar{f}_k^{l+r-2} \cos \left((r-l) \frac{\bar{a}_k}{\bar{f}_k} \right) \right), \quad (2.12) \end{aligned}$$

Here V_s is part of the potential that preserves the shift symmetry and V_{sb} is the part that breaks the shift symmetry. We note that because of the periodic nature of the potential, Eqs.(2.10-2.12) provide a valid theory even for $a_i > M_{Pl}$.

Next we look at the mass matrix for the axions. The mass matrix consists of three types of terms: $M(a_l, a_p)$ which involves only the axions $a_i, i = 1, \dots, m$, $M(\bar{a}_l, \bar{a}_p)$ which involves only the axions $\bar{a}_i, i = 1, \dots, m$, and the matrix with the cross terms $M(a_k, \bar{a}_p)$. For the computation of the heavier axion masses it is sufficient to look at the mass matrix in the limit when shift symmetry breaking is absent, i.e., ignore V_{sb} , and inclusion of the breaking of the shift symmetry would make only negligible contribution to the heavy axion masses. An explicit computation of these gives the following: For $M(a_l, a_p)$ one has

$$M(a_l, a_p) = 2\delta_{lp} \frac{1}{f_p^2} \left(\sum_{k=1}^m \mu_{pk} \bar{f}_k \right)^2 + 2 \sum_{k=1}^m \left(\mu_{lk} + 2 \frac{\lambda_{lk}}{M} \bar{f}_k f_l \right) \left(\mu_{pk} + 2 \frac{\lambda_{pk}}{M} \bar{f}_k f_p \right). \quad (2.13)$$

For $M(\bar{a}_l, \bar{a}_p)$ one has

$$M(\bar{a}_l, \bar{a}_p) = 2\delta_{lp} \frac{1}{\bar{f}_p^2} \left(\sum_{k=1}^m \mu_{kp} f_k \right)^2 + 2 \sum_{k=1}^m \left(\mu_{kl} + 2 \frac{\lambda_{kl}}{M} f_k \bar{f}_l \right) \left(\mu_{kp} + 2 \frac{\lambda_{kp}}{M} f_k \bar{f}_p \right), \quad (2.14)$$

and for the cross term $M(a_k, \bar{a}_p)$ one has

$$M(a_k, \bar{a}_p) = M(\bar{a}_p, a_k) = -2 \sum_{l=1}^m \left(2 \frac{\lambda_{kp}}{M} (\mu_{kl} \bar{f}_l \bar{f}_p + \mu_{lp} f_l f_k) - \mu_{kp} \left(\frac{\lambda_{kl}}{M} \bar{f}_l^2 + \frac{\lambda_{lp}}{M} f_l^2 \right) \right) \quad (2.15)$$

This mass matrix is $2m \times 2m$ dimensional. It has $2m - 1$ non-zero eigenvalues and one eigenvalue is identically zero which corresponds to the inflaton. This result is a consequence of the Goldstone theorem[48] which requires that the spontaneous breaking of a single global $U(1)$ symmetry leads to a single massless Goldstone mode which implies that there is just one possibility for the inflation field which is the zero mode in the diagonalization of a $2m \times 2m$ matrix as noted above and all other modes are heavy after spontaneous breaking.

3 The axion landscape and a Fast roll-Slow roll splitting mechanism

As discussed in the preceding section, even though we have a landscape of axions, i.e., pseudo scalar fields, there is only one $U(1)$ shift symmetry and correspondingly there is only one linear combination of the axion fields which is the pseudo-Nambu-Goldstone-boson and acts as the inflation field. The reduction of the multi axion system to a single inflation field does not mean that one has the same dynamics if one started with a single field. The reason for this is the follows: our starting point was a landscape of axions each of which undergoes a shift under the same $U(1)$. The inflation field thus includes pieces of each of these fields. Further, although in the limit of no breaking of the shift symmetry, the dynamics of the (pNGB) inflaton is decoupled from the rest of the axions, there is mixing between the two sectors once the shift symmetry is broken. In this case the diagonalization will yield $2m - 1$ massive axions and a relatively lighter inflation field. In principle all the axions both light and heavy enter in inflation, except that the $2m - 1$ axions produce a fast roll and die off relatively quickly while the inflation field produces the slow roll. To check that the multi-field analysis is faithfully reproduced by the effective single field, we carry out a numerical analysis for a multi-field case and compare the result to that for the effective single field and find that the fast roll-slow roll decomposition is justified. We emphasize that the assumption of only one global symmetry will automatically result in only one inflation direction and one inflation candidate and all other axions will be heavy. After the breaking of the shift symmetry, the potential for the axions will in general be mixed involving all the axions. We discuss below the explicit procedure for the splitting of the total potential given by Eqs.(2.10-2.12) into the fast roll-slow roll parts.

The potential of Eqs.(2.10-2.12) contains two parts: V_s and V_{sb} where V_s is part of the potential that preserves the shift symmetry and V_{sb} is the part that breaks the shift symmetry. Eqs.(2.10-2.12) contain a mixture of fast roll and slow roll parts. We wish to decompose Eqs.(2.10-2.12) to extract the slow roll part. There are $2m$ number of axionic fields a_1, \dots, a_m and $\bar{a}_1, \dots, \bar{a}_m$. Since there is only one $U(1)$ shift symmetry, we can pick a basis where only one linear combination of it is variant under the shift symmetry and all others are invariant. We label this new basis $b_-, b_+, b_1, b_2, \dots, b_{m-1}, \bar{b}_1, \bar{b}_2, \dots, \bar{b}_{m-1}$ where only b_- is sensitive to the shift symmetry. An explicit exhibition of this basis is below

$$\begin{aligned}
b_k &= \frac{a_{k+1}}{f_{k+1}} - \frac{a_1}{f_1}, \quad k = 1, 2, \dots, m-1, \\
\bar{b}_k &= \frac{\bar{a}_{k+1}}{\bar{f}_{k+1}} - \frac{\bar{a}_1}{\bar{f}_1}, \quad k = 1, 2, \dots, m-1, \\
b_+ &= \frac{a_1}{f_1} + \frac{\bar{a}_1}{\bar{f}_1}, \\
b_- &= \frac{1}{\sqrt{\sum_{k=1}^m f_k^2 + \sum_{k=1}^m \bar{f}_k^2}} \left(\sum_{k=1}^m f_k a_k - \sum_{k=1}^m \bar{f}_k \bar{a}_k \right). \tag{3.1}
\end{aligned}$$

Thus the first three equations in Eq.(3.1) give us $2(m-1)+1 = 2m-1$ linear combinations of axionic fields which are invariant under the shift symmetry while the last one gives us the combination of axionic fields which is sensitive to shift symmetry. It can be easily checked that b_- is orthogonal to all the rest, i.e.,

$$(b_-, b_k) = 0 = (b_-, \bar{b}_k), \quad (b_-, b_+) = 0, \quad k = 1, 2, \dots, m-1. \tag{3.2}$$

We identify b_- as the inflaton since in the absence of breaking of the shift symmetry it is massless while the remaining $(2m-1)$ fields $b_+, b_k, \bar{b}_k, k = 1, \dots, m-1$ are massive. Thus the slow roll is controlled by b_- only. Accordingly one can decompose the scalar potential into two parts, V_{fast} and V_{slow} where

$$V(b, \bar{b}) = V_{\text{fast}}(b_+, \{b_k\}, \{\bar{b}_k\}) + V_{\text{slow}}(b_-), \quad k = 1, \dots, m-1. \tag{3.3}$$

While both V_{fast} and V_{slow} can be computed from Eqs.(2.10-2.12), here we focus on V_{slow} . The following projections are useful in extracting the slow roll part of the potential

$$\begin{aligned}
\left(b_-, (r-1) \frac{a_k}{f_k} - \frac{\bar{a}_l}{\bar{f}_l} \right) &= \frac{r}{f_e}, & \left(b_-, (r-1) \frac{\bar{a}_k}{\bar{f}_k} - \frac{a_l}{f_l} \right) &= -\frac{r}{f_e}, \\
\left(b_-, (r-2) \frac{a_k}{f_k} - 2 \frac{\bar{a}_l}{\bar{f}_l} \right) &= \frac{r}{f_e}, & \left(b_-, (r-2) \frac{\bar{a}_k}{\bar{f}_k} - 2 \frac{a_l}{f_l} \right) &= -\frac{r}{f_e}, \\
\left(b_-, (r-l) \frac{a_k}{f_k} \right) &= \frac{r-l}{f_e}, & \left(b_-, (r-l) \frac{\bar{a}_k}{\bar{f}_k} \right) &= \frac{-r+l}{f_e},
\end{aligned} \tag{3.4}$$

where

$$f_e = \sqrt{\sum_{k=1}^m f_k^2 + \sum_{k=1}^m \bar{f}_k^2}. \tag{3.5}$$

Using Eq.(3.4) in Eq.(2.12), and using Eq.(2.9) to eliminate λ , one finds

$$\begin{aligned}
V_{\text{slow}}(b_-) &= \sum_{k=1}^m \left[2 \sum_{r=1}^q r \left(A_{kr} f_k^{r-1} \sum_{l=1}^q l A_{kl} f_k^{l-1} + \bar{A}_{kr} \bar{f}_k^{r-1} \sum_{l=1}^q l \bar{A}_{kl} \bar{f}_k^{l-1} \right) \times \right. \\
&\quad \left(1 - \cos \left(\frac{r}{f_e} b_- \right) \right) - 2 \sum_{l=1}^q \sum_{r=l+1}^q l r \left(A_{kl} A_{kr} f_k^{l+r-2} + \bar{A}_{kl} \bar{A}_{kr} \bar{f}_k^{l+r-2} \right) \\
&\quad \left. \times \left(1 - \cos \left(\frac{r-l}{f_e} b_- \right) \right) \right]. \tag{3.6}
\end{aligned}$$

A remarkable aspect of Eq.(3.6) is that the cosine functions depend only on an effective decay constant f_e . Thus for the $2m$ number of fields, if we set $f_k = f = \bar{f}_k$, we have $f_e = \sqrt{(2m)}f$ which means that even with f sub-Planckian we can get the effective f_e much larger than M_{Pl} if we choose m large enough. We note that if we set $f_k = f = \bar{f}_k$, and $N = 2m$, Eq.(3.5) takes the form $f_e = \sqrt{N}f$ which is similar to what one has in the case of N-flation [20]. However, the inflation potential arising from the fast roll-slow roll splitting is very different from the one in N-flation. The implication of Eq. (3.5) and its simplified version $f_e = \sqrt{N}f$ is the following: by inclusion of more fields the range of the axion decay constant consistent with inflation is enlarged which increases the allowed parameter space of the theory. Specifically the region of the sub-Planckian domain of the axion decay constant is significantly enlarged. One generally expects this result in the reduction of the type described above, see, e.g., Eq.(3.18) of [85].

4 Extension to supergravity

Next we extend the analysis to supergravity where the scalar potential has the form [49, 50]

$$V = e^K [D_i W K_{ij}^{-1} D_j^* W^* - 3|W|^2] + V_D, \quad (4.1)$$

Here K is the Kähler potential and W , as in global supersymmetry, is the superpotential. Further,

$$D_i W = \frac{\partial W}{\partial \phi_i} + \frac{\partial K}{\partial \phi_i} W. \quad (4.2)$$

The D -term of the potential, V_D , will play no role in our analysis and we omit it from here on. Now in supergravity there is the well known η problem (see Appendix B for the definition of η) which arises because the Kähler potential contributes to η and this contribution can be $O(1)$ while for slow roll inflation one needs $\eta \ll 1$. To avoid the η problem we will use the following form for the Kähler potential, i.e.,

$$K = \sum_i \frac{1}{2} (S_i + S_i^\dagger)^2, \quad (4.3)$$

We consider here for simplicity a single pair of axions with opposite shift symmetries. We parametrize the complex scalar component ϕ_i of $S_i, i = 1, 2$ so that

$$\phi_i = (\rho_i + ia_i)/\sqrt{2}, \quad i = 1, 2, \quad (4.4)$$

where a_i have the shift property

$$a_1 \rightarrow a_1 + \lambda, \quad a_2 \rightarrow a_2 - \lambda, \quad (4.5)$$

and ρ_i are the saxion fields. In this case it is easily checked that the kinetic energy is given by

$$L_{kin} = -\frac{1}{2} [\partial_\mu \rho_i \partial^\mu \rho_i + \partial_\mu a_i \partial^\mu a_i], \quad (4.6)$$

so the fields a_i and ρ_i are canonically normalized. The superpotential is chosen to be of the form

$$\begin{aligned} W &= W_s + W_{sb}, \\ W_s &= \frac{1}{2}\mu(S_1 + S_2)^2 + \frac{1}{3}\lambda(S_1 + S_2)^3 + W_0, \\ W_{sb} &= P(S_1) + P(S_2), \end{aligned} \quad (4.7)$$

where W_0 arises from a hidden sector. For supergravity analysis the saxion can be stabilized by imposition of spontaneous symmetry breaking conditions [51] $D_i W = 0, i = 1, 2$ which give

$$\sqrt{2}\mu f + 2\lambda f^2 + P' \left(\frac{f}{\sqrt{2}} \right) + \sqrt{2}f\alpha = 0 \quad (4.8)$$

where

$$\alpha = \mu f^2 + \frac{2\sqrt{2}}{3}\lambda f^3 + 2P \left(\frac{f}{\sqrt{2}} \right) + W_0, \quad (4.9)$$

while the vanishing of the vacuum energy after the inflationary period gives the additional constraint $\alpha = 0$. For shift symmetry breaking we assume $P = \sum_n A_n e^{c_n S}$ so that

$$W_{sb} = \sum_{n=1}^q A_n (e^{c_n S_1} + e^{c_n S_2}). \quad (4.10)$$

Next we choose a new basis for the axions, where we replace a_1, a_2 by b_+, b_- so that

$$b_{\pm} = \frac{1}{\sqrt{2}}(a_1 \pm a_2). \quad (4.11)$$

where b_+ is invariant under the shift symmetry while b_- is sensitive to the shift symmetry. As in the global supersymmetry case the computation of the inflation potential is carried out by expanding around the minimum of the saxion potential. Further, we retain only the slow roll part of the potential which involves b_- . In this case W_{sb} takes the form

$$W_{sb} = - \sum_{n=1}^q B_n (e^{i\gamma_n \frac{b_-}{\sqrt{2}f}} + e^{-i\gamma_n \frac{b_-}{\sqrt{2}f}}). \quad (4.12)$$

where $B_n = -A_n e^{c_n f/\sqrt{2}}$ and $\gamma_n = c_n f/\sqrt{2}$. In this case, after stabilization of the saxions and imposition of a vanishing vacuum energy at the end of inflation, and using the fast roll-slow roll splitting mechanism we get the following potential for the inflation field

$$\begin{aligned} V(b_-) &= e^{2f^2} \left[2 \sum_{n=1}^q \sum_{m=1}^q c_n c_m B_n B_m \left(1 - 2 \cos\left(\frac{\gamma_n b_-}{\sqrt{2}f}\right) + \cos((\gamma_n - \gamma_m) \frac{b_-}{\sqrt{2}f}) \right) \right. \\ &\quad + \sum_{n=1}^q \sum_{m=1}^q (16f^2 + 8\sqrt{2}f c_n - 12) B_n B_m \left(1 - \cos(\gamma_n b_-/\sqrt{2}f) - \cos(\gamma_m b_-/\sqrt{2}f) \right. \\ &\quad \left. \left. + \frac{1}{2} \cos((\gamma_n - \gamma_m) b_-/\sqrt{2}f) + \frac{1}{2} \cos((\gamma_n + \gamma_m) b_-/\sqrt{2}f) \right) \right]. \end{aligned} \quad (4.13)$$

As noted in the beginning, the analysis above is for one pair of axionic chiral fields. As in the global supersymmetry case the analysis can be extended to m pairs of axionic chiral fields. Again as for the global supersymmetry case this extension would modify the effective axion decay constant for the inflation field so that $\sqrt{2}f$ is replaced by $\sqrt{2mf}$.

5 Consistency with Planck data [10, 11]

5.1 Experimental observables

The path for testing inflationary models with experimental data from the cosmic microwave background (CMB) radiation anisotropies has been well laid out in the literature. The central quantities that enter are the correlation functions involving scalar and tensor perturbations of the inflaton and of the gravitational field which are coupled. From the correlation functions one deduces the power spectrum for curvature perturbations and the power spectrum for tensor perturbations and the spectral indices. These are the quantities which are experimentally measured. A brief description of these is given in section 8 which also defines the notation we use in this section, i.e., $\mathcal{P}_{\mathcal{R}}$ for the power spectrum for comoving curvature perturbations, \mathcal{P}_t for the power spectrum for tensor perturbations, and n_s , n_t for the scalar and tensor spectral indices. Inflationary models typically exhibit the power law behavior $\mathcal{P}_{\mathcal{R}} \propto k^{n_s-1}$ and $\mathcal{P}_t \propto k^{n_t}$. The power spectrum for the curvature perturbations can be expanded around the pivot scale k_0 , where the pivot scale is the scale chosen for carrying out the analysis, so that

$$\begin{aligned}\mathcal{P}_{\mathcal{R}}(k) &= \mathcal{P}_{\mathcal{R}}(k_0) \left(\frac{k}{k_0}\right)^{n_s(k)-1}, \\ n_s(k) &= n_s(k_0) + \frac{1}{2} \left(\frac{dn_s}{d\ln k}\right) \ln\left(\frac{k}{k_0}\right).\end{aligned}\tag{5.1}$$

Similarly for the tensor perturbations we have

$$\begin{aligned}\mathcal{P}_t(k) &= \mathcal{P}_t(k_0) \left(\frac{k}{k_0}\right)^{n_t(k)}, \\ n_t(k) &= n_t(k_0) + \frac{1}{2} \left(\frac{dn_t}{d\ln k}\right) \ln\left(\frac{k}{k_0}\right).\end{aligned}\tag{5.2}$$

One also defines a quantity r which is the ratio of the tensor to scalar power spectrum so that

$$r = \frac{\mathcal{P}_t(k_0)}{\mathcal{P}_{\mathcal{R}}(k_0)},\tag{5.3}$$

The current experimental limits from Planck experiment at $k_0 = 0.05 \text{ Mpc}^{-1}$ are as follows [10–12]

$$\begin{aligned}n_s &= 0.9645 \pm 0.0049 \text{ (68\%CL)} \\ r &< 0.07 \text{ (95\%CL)}\end{aligned}\tag{5.4}$$

while $n_t(k_0)$ is currently not constrained. As discussed in Appendix B (sec. (8)) the spectral indices can be related to the slow roll parameters ϵ and η (see Eq.(8.23)). Here we will focus on the computation of the spectral indices as these are directly measured. Further, one requires the number of e-foldings to be in the range $N_e = [50, 60]$ where N_e is the number of e-foldings between the horizon exit and the end of inflation, i.e., $N_e = N_{\text{total}} - N_{\text{exit}}$, where N_{exit} is the number of e-foldings at horizon exit and N_{total} is the total number of e-foldings at the end of inflation. For a mode k , horizon exit occurs at time when $k = RH = \dot{R}$ and the Hubble radius is $(RH)^{-1}$. To test our model with Planck data we use the code of [53] which is suitable for multi field inflation models. We have checked this code for simple potentials by a direct integration of the Friedman equations for an inflaton field (see Appendix A). The code provides the spectral indices n_s, n_t and the ratio of the tensor to scalar power spectrum.

5.2 Monte Carlo Analysis for fit to data

In this subsection we carry out a Monte Carlo analysis on the parameter space of the models we consider. First we consider the model of Eq.(3.6). However, we will make some simplifying assumptions in the analysis which are: $A_{kl} = \bar{A}_{kl} = B_l f^{3-l}$, $B_l = BG_l$, $f_k = f$ for all k . Thus B_l, B, G_l are dimensionless while $f_k = f$ carry dimension of mass. Let us take the potential of Eq.(3.6) and simplify it using these assumptions which gives

$$V_{\text{slow}}(b_-) = 4mf^4 B^2 \left(\sum_{l=1}^q l G_l \sum_{r=4}^q r G_r \left(1 - \cos \left(\frac{r}{\sqrt{2m}} \frac{b_-}{f} \right) \right) - \sum_{l=1}^q \sum_{r=l+4}^q l r G_l G_r \left(1 - \cos \left(\frac{r-l}{\sqrt{2m}} \frac{b_-}{f} \right) \right) \right). \quad (5.5)$$

Thus Eq.(5.5) is the simplified version of Eq.(3.6). We remind the reader that in Eq.(5.5), m is the number of axion pairs where the two axions in each pair have opposite $U(1)$ shift symmetry, and q is the highest power in the polynomial that breaks the shift symmetry. We assume that the terms in the polynomial that break the shift symmetry are operators with dimension higher than 3 in the superpotential. Thus we assume that r takes on the values in the range $[4, q \geq 4]$.

Before embarking on a full Monte Carlo analysis we wish to test the accuracy of the fast roll-slow roll decomposition. As shown in sections 3 and 4, the procedure of decomposing the axion potential into fast roll and slow roll parts brings in a huge simplification in the analysis. We need to verify, however, that neglecting the fast roll part of the potential is a valid approximation. For that we consider a simple case where we compute spectral indices using the full potential including slow roll and fast roll and then just the slow roll by itself. The case we consider is when we have just one pair of axions, i.e., $m = 1$, and we consider a single term in the polynomial that breaks the shift symmetry, i.e., we take just the term G_4 . Further we set $G_4 = 1$ since it can be absorbed in the parameter B . The analysis is done in high precision to exhibit the difference between the two cases. The example we choose is taken from a Monte Carlo analysis and the model point satisfies the Planck data constraints. However, $f > M_{Pl}$ in the example below, but this can be easily alleviated by choosing $m > 1$

and the decay constant $f' = f/\sqrt{m}$. Here we first run the slow-roll part of the potential. The specific parameters here are $f = 14.9605M_{Pl}$, $b_{-,0} = 13.963M_{Pl}$, and $N_{\text{pivot}} = 56$. In this case, $n_s = 0.953167 \pm 0.000007$, $n_t = -0.005756 \pm 0.000007$, $r = 0.044045984 \pm 0.000000003$, where errors were computed by varying the number of subhorizon e-foldings in the integration. Next, we run the full (both slow and fast) simulation with $\mu = M_{Pl}$, $B = 10^{-4}$, and $a_1 = (b_{-,0} + 13M_{Pl})/\sqrt{2}$, $\bar{a}_1 = (-b_{-,0} - 13M_{Pl})/\sqrt{2}$. Here one finds that N_{total} increases from 79.2 to 126.0 due to the presence of the fast roll part. However, the inflation observables in this case are: $n_s = 0.953169 \pm 0.000006$, $n_t = -0.005754 \pm 0.000006$, and $r = 0.044045988 \pm 0.000000010$. As one can see the accuracy of slow-roll fast-roll decomposition surpasses the precision of the integration. We further compare these results to the answers obtained with a slow-roll approximation, from which we get $\epsilon = 0.00288$, $\eta = -0.0150$, $r = 0.04604$, $n_s = 0.9527$, $n_t = -0.005755$. As one can see apart from n_t the discrepancy is now significantly larger than the integration precision. We get $\delta r = 0.002$, $\delta n_s = 0.0005$, $\delta n_t = 0.000001$ comparing to the single-field simulation. However, while the n_t value is extremely close to the slow roll prediction, there is a deviation in the value of r . Thus more precise measurement of r , would allow a test for deviation from the slow roll relation $n_t + r/8 = 0$.

Similarly, for a supergravity example on Fig.(7), we get $r = (1.03994375 \pm 0.00000002) \times 10^{-4}$, $n_s = 0.9724973 \pm 0.0000007$, $n_t = (-1.29 \pm 0.07) \times 10^{-5}$. On the other hand, from slow-roll approximation we get, $r = 1.07 \times 10^{-4}$, $n_s = 0.9714$, $n_t = -1.34 \times 10^{-5}$. Here, both values of r are way below experimental limit (as is true for most cases on Fig.(10)), $\delta n_s = 0.0011$, which is 22% of the experimental limit, and the difference for n_t is smaller than the simulations precision.

A comparison of fast roll vs slow roll is given in Fig.(1). Here the left panel gives the fast and the slow field components as a function of the number of e-foldings. The right panel gives a comparison of the energy of the slow field and the energy of the fast field components as a function of the number of e-foldings. One finds that the fast component starts with a larger energy, but the slow component overtakes it and drives inflation. In Fig.(2) we give the fast and the slow field components as a function of time in the left panel. On the right panel we display the energy of the slow field and of the fast field as a function of time. We note that the fast field component dies about a factor of 100 faster than the slow component in this case. Similar behavior generally occurs in both global supersymmetry and supergravity models as long as the slow-roll part of the potential is much smaller than the fast-roll part. For that reason we disregard the fast-roll part in the further analysis, and perform simulations with the slow-roll part only.

We proceed now to discuss the result of the full Monte Carlo analysis of the parameter space of Eq.(5.5). In the left panel of Fig.(3) we give an analysis of r vs n_s for the parameter space when $G_4 = 1$, $G_5 \neq 0$. The scatter plot is on the Planck data where the blue region corresponds to 68% and 95% CL regions of Planck TT, TE, EE + lowP in Fig. (11) of [11]. One finds that there are a large number of parameter points in the region in r vs n_s allowed by the Planck experiment. The black dots and the green dots correspond to scenarios where b_- reaches global minimum at the end of inflation. The scatter points have a mixture of axion decay constant both below and above the Planck mass. In the right panel we exhibit

the data set where $f < M_{Pl}$. We note in passing that the parameter points in the left panel where $f > M_{Pl}$ may be reduced to lie below M_{Pl} by choosing the appropriate number of axion pairs m .

Next we extend our result to include $G_6 \neq 0$. The analysis enlarges the number of allowed models which pass all the experimental tests and have $f < M_{Pl}$. We do this by starting with the parameter points passing experimental tests from the analysis of Fig.(3) and extending the region corresponding to these points into $G_6 \neq 0$ region. The analysis shows that the inflation trajectory is a narrow strip in the (G_5, G_6) plane as shown in Fig.(4). In Fig.(5) we give the distribution in (n_s, r) for the parameter space of Fig.(4). We note that here $N_{\text{pivot}} = [50, 60]$, the full set of the parameter points pass the experimental constraints on n_s and r and the parameter points have $f < M_{Pl}$. In Fig.(6) we give the distribution of n_t vs. n_s for the same parameter space as for Fig.(5). Currently there is no experimental data on n_t and thus the distribution in the (n_s, n_t) plane is a prediction which may be tested in future experiments. Clearly a constraint on n_t will narrow down the range of the parameter space further. Here we note that the inflationary trajectory which lies in a narrow strip in the (G_5, G_6) plane in Fig.(4) indicates that inflation with desired properties does not arise for random choices of parameters but occurs along a constrained path in the (G_5, G_6) plane. Thus inflation is a fine tuned phenomenon. Part of the reason for fine tuning is the following: while inflation with a number of e-foldings can arise for a much larger parameter space, the parameter space gets successively reduced as one imposes the constraint on $N_{\text{pivot}} = [50, 60]$, and the constraint on n_s and on r (see, e.g., Fig.(3)). In other words one does not expect that any random choice of parameters will result in the desired number of e-foldings and with n_s and r consistent with experiment. Thus inflation occurs in small patches of the parameter space but the number of such patches is very large. A similar phenomenon occurs in electroweak symmetry breaking in supergravity models [61] where the constraints of color and charge conservation, relic density constraints and the constraint to have the Z -mass to be the experimental value significantly reduce the parameter space of supergravity models. We note in passing that all the parameter points exhibited in Figs.(3)-(6) satisfy the Lyth bound [62] for slow roll inflation, i.e.,

$$\frac{\Delta\phi}{M_{Pl}} \geq \left(\frac{r}{0.01}\right)^{1/2}, \quad (5.6)$$

where $\Delta\phi = (\phi_{\text{end}} - \phi_{\text{exit}})$. We also note in passing that the inflaton mass in the cases considered above is $O(10^{-4})M_{Pl}$. With reference to Fig.(4) we note that the purpose of the analysis is to present one concrete example of a trajectory which supports inflation consistent with data but there could be other trajectories which do the same. The generation of such trajectories is computer intensive and a dedicated computer analysis would be needed to exhaust all the allowed regions where inflation can occur.

Finally we give the Monte Carlo analysis for the supergravity model of Eq.(4.13). We begin by displaying in Fig.(7) a generic potential for b_- for the supergravity case when $m = 1$ (see Eq.(4.13)). Next for the same parameter set as used in Fig.(7) we exhibit the

phenomenon of fast roll and slow roll in Fig.(8). Thus in Fig.(8) the left panel gives the evolution of the fast component (blue) and of the slow component (red) as a function of time, while the right panel gives the energy of the fast (blue) and the slow (red) component as a function of time. As in the global supersymmetry case here too one finds that the fast component dies about a hundred times faster than the slow component and thus the slow component rules inflation. To test the model with experiment, we note that for the case $q = 1$, the desired number of e-foldings are not achieved, while for the case $q = 2$ one can get the right number of e-foldings but not the desired values of n_s . However, the case $q = 3$ gives consistent inflation. Here we investigate the range of the parameter space where $A_1 = M_{Pl}^2$, $A_2/A_1 = [-1, 1]$, $A_3/A_2 = [-1, 1]$, $f/M_{Pl} = [0, 1]$. In Fig.(9) we exhibit the parameter space which gives rise to consistent inflation. The left panel displays the parameter space in the A_3/A_1 vs. A_2/A_1 plane and the right panel exhibits the parameters space in the f vs. A_2/A_1 plane. As can be seen in this panel all the parameter space exhibited has f lying in the sub-Planckian region. In the left panel of Fig.(10) we give the prediction of r vs n_s and in the right panel a prediction of n_t vs n_s . In Figs.(9) and (10) the green and the black points have the same meaning as in Fig.(3). As in global supersymmetry case, here too all the parameter points exhibited in Figs.(9)-(10) satisfy the Lyth bound [62].

The analysis given above shows that the effective theory does not automatically lead to the exact standard single-field inflation results but the predictions of the model lie very close to them. For example, in one of the cases considered above one finds deviations from the standard single-field case so that $\delta r = 0.002$, $\delta n_s = 0.0005$ and $\delta n_t = 0.000001$. Thus as stated earlier although the n_t value is very close to the slow roll prediction, there is a deviation in the value of r and a more precise measurement of r would allow a test for deviation from the slow roll relation $n_t + r/8 = 0$.

5.3 Generation of a flat inflation potential

In this section we give further details on the generation of a locally flat scalar potential arising from the instanton induced axion superpotential. In supersymmetric models symmetry breaking terms are added in the superpotential with coefficients which are exponentially suppressed. For q number of symmetry breaking terms induced by instantons in the superpotential, there are in general $n = 2q$ number of cosines with different periods in the scalar potential which follows from the simple relationship between the scalar potential and the superpotential. Further, the coefficients of the cosines contain products of suppression factors because the scalar potential generates cross-terms which automatically arise in going from the superpotential to the scalar potential as can be seen from Eq.(38) where a double sum appears on the cosines and their coefficients. Such cross terms are relevant in generating a local flatness of the scalar potential. To illustrate this point more clearly we exhibit in Appendix C (section 9) the analytic expression for the scalar potential for the case $m = 1, q = 3$ relevant for Fig. 7. First, we note that in this case one has six cosines which are of the form $\cos(\frac{nb}{\sqrt{2}f})$, $n = 1, \dots, 6$ and we have displayed the suppression factors for each of the six cosines in Eq. (72). In Eq. (72) $A_i, i = 1, 2, 3$ are the suppression factors and we see that products of them appear in all six cosines. Thus A_1 appears in the first

four, A_2 appears in the first five and A_3 appears in the coefficients of all six cosines. In Eq.(73) we give the numerical sizes of the coefficients of the cosines for the case of Fig. 7. Here we note that for the case when

$$\frac{b}{\sqrt{2}f} = \pi$$

(which corresponds to $b = 3.65$ for $f = 0.8211$ used in Fig.7) the terms in the first, the third and the fifth brace in Eq.(73) give maximum contributions while the contributions of the terms in the second, the fourth and the sixth brace vanish. Thus we see three sets of terms going through a maximum and the other three going through a minimum. With reference to Fig. 7, we see that indeed the first cosine term is going through its maximum while the second cosine is going through its minimum at $b = 3.65$. The higher cosine terms are following similar patterns although their contributions are relatively small. A superposition of these leads to a local flatness around the point where the maxima and the minima simultaneously occur. This can be roughly seen by just superposing the first two dominant terms in Eq. (73) which appear as the green curve and the brown curve in Fig. 7. Further from Eq.(73) one can also understand the size of the potential in the region of flatness.

We note in passing that a similar procedure of using several non-perturbative terms to produce inflation by adjustment of parameters in the non-perturbative terms is used in the so-called ‘racetrack’ models (see, e.g., [66–80] and for related works [81–84]). In our analysis the shift symmetry produces a flat direction and its breaking reduces the shift symmetry from a continuous to a discrete one. The breaking produces a specific combination of cosines with different periods which leads to local flatness in the potential at points where the maxima of one set of cosines overlaps with the minima of the other set of cosines.

6 Conclusion

We have investigated models of multi-field inflation when there is an underlying $U(1)$ shift symmetry. We have proposed a new technique, the fast roll-slow roll splitting mechanism, which involves a decomposition of the inflation potential into two parts: a fast roll part and a slow roll part. The technique was tested and found to be highly accurate. The fast roll-slow roll decomposition reduces the problem of multi-field inflation to that of a single field inflation and is likely to be realized in string theory because of the possible existence of many axions with $U(1)$ symmetry in strings. We have applied this technique for the analysis of spectral indices for an inflation model in a supersymmetric axionic landscape. The breaking of the shift symmetry was accomplished by instanton inspired terms in the superpotential. It is found that a large part of the parameter space exists where a number of e-foldings in the range $[50, 60]$ are accomplished. This parameter space is reduced on imposing the experimental limit on the spectral index n_s of curvature perturbations and the limit on the ratio of the power spectrum of tensor perturbations to the power spectrum of curvature perturbations. Further, in the analysis we show that inflation, which satisfies all experimental constraints, can be achieved with sub-Planckian values of the decay constant

which is a significant result of the analysis. It is found that the axion landscape model can reach most of the allowed region of experiment for the spectral indices. The model allows the inflaton field to have initial values which lie in the super-Planckian region and thus there is a possibility of gravitational waves during the inflationary period. Among other topics of interest is the heating after inflation (for a recent review see [63]) and a variety of associated phenomena such as non-Gaussianities in the curvature perturbations, generation of primordial black holes and of primordial magnetic fields, and baryogenesis. These are topics worthy of study within the well defined framework presented in this work which is a model with stabilized saxions and supports inflation consistent with all of the current experimental constraints. Since strings are the most natural framework where axionic landscape can occur, it would be natural to extend this analysis to strings which should be an interesting topic of investigation in the future a realistic analyses could be done with stabilized moduli as in [64, 65].

Acknowledgments

Conversations with Jim Halverson, Cody Long and Fernando Quevedo are acknowledged. This research was supported in part by the NSF Grant PHY-1620575.

7 Appendix A: Preliminaries

As our starting point we assume homogeneity on cosmological scales, so that the metric takes the form

$$ds^2 = -dt^2 + R(t)^2 (dx^2 + dy^2 + dz^2) ,$$

where $R(t)$ is the scale factor. For $2m$ number of axionic fields, the Lagrangian is given by

$$\mathcal{L} = -\frac{1}{2} \sum_{a=1}^{2m} (\partial_\mu \phi_a \partial^\mu \phi_a) - V(\phi) . \quad (7.1)$$

In this case the two Friedman equations are

$$\begin{aligned} 3M_{Pl}^2 \frac{\dot{R}^2}{R^2} &= \frac{1}{2} \dot{\phi}_a \dot{\phi}_a + V(\phi) , \\ -2M_{Pl}^2 \frac{\ddot{R}}{R} - M_{Pl}^2 \frac{\dot{R}^2}{R^2} &= \frac{1}{2} \dot{\phi}_a \dot{\phi}_a - V(\phi) . \end{aligned} \quad (7.2)$$

Further the field equations give us

$$\ddot{\phi}_a + 3 \frac{\dot{R}}{R} \dot{\phi}_a = - \frac{\partial V}{\partial \phi_a} . \quad (7.3)$$

Let us define the number of e-foldings N so that $N = \ln(R/R_0)$, where R_0 is the value of R at the beginning of inflation. One can derive the following equations for N from the Friedman equations Eqs.(7.2) and the field equation Eq.(7.3)

$$\begin{aligned}
3M_{Pl}^2\dot{N}^2 &= \frac{1}{2}\dot{\phi}_a\dot{\phi}_a + V(\phi) , \\
\ddot{\phi}_a + 3\dot{N}\dot{\phi}_a &= -\frac{\partial V}{\partial\phi_a} .
\end{aligned} \tag{7.4}$$

Integration of these equations allows for a determination of the axion fields as a function of the number of e-foldings and also as a function of time.

8 Appendix B: Power spectrum and Spectral Indices

To test the inflation model with Planck data [10, 11] we need to compute the power spectrum of curvature and tensor perturbations and spectral indices. A brief discussion is given here to define notation and make the numerical analysis more comprehensible, and more exhaustive treatments can be found in several reviews [54–57]. Let us begin by considering a massless scalar field within a gravitational background so that

$$\mathcal{A}_\phi = \int d^4x \sqrt{-g} \left(-\frac{1}{2} \partial_\mu \phi \partial^\mu \phi \right) . \tag{8.1}$$

It is found convenient to use the conformal time ζ so that

$$\zeta = \int \frac{dt}{R(t)} . \tag{8.2}$$

Perturbations of the inflaton field should be considered along with the perturbations of the gravitational field. The general linear perturbations of the FRW metric can be parametrized as

$$ds^2 = R^2 \left[- (1 + 2\alpha) d\zeta^2 + 2\beta_i dx^i d\zeta + (\delta_{ij} + h_{ij}) dx^i dx^j \right] , \tag{8.3}$$

where α, β_i, h_{ij} parametrize the perturbations. These perturbations can be decomposed into scalar, vector and tensor components. For β_i we have

$$\beta_i = \nabla_i \beta + \beta'_i , \quad \nabla_i \beta'^i = 0 . \tag{8.4}$$

where β is the scalar and β'_i the vector component. We decompose h_{ij} so that

$$\begin{aligned}
h_{ij} &= 2\gamma\delta_{ij} + 2\nabla_i \nabla_j \kappa + 2\Delta_{(i} \kappa_{j)} + \kappa_{ij} , \\
\nabla_i \kappa^{ij} &= 0 , \quad \kappa^{ij} \delta_{ij} = 0 .
\end{aligned} \tag{8.5}$$

First we consider the scalar perturbations. It turns out that the scalar perturbation of interest is given by the combination

$$\sigma = R \left(\delta\phi - \gamma \frac{\phi'}{\mathcal{H}} \right) , \tag{8.6}$$

where the prime on ϕ stands for derivative of ϕ with respect to the conformal time ζ and \mathcal{H} is the Hubble parameter in conformal time. Here σ is a combination of the scalar field and metric perturbations and is gauge invariant. The quadratic part of action for σ is given by

$$\mathcal{A}_\sigma \simeq \frac{1}{2} \int d\zeta d^3x \left[\sigma'^2 + \vec{\nabla}\sigma \cdot \vec{\nabla}\sigma + \frac{z''}{z} \sigma^2 \right] , \tag{8.7}$$

where $z = R\phi'/\mathcal{H}$. In the slow roll approximation one has $z''/z \simeq R''/R$. Thus Eq.(8.7) takes the form

$$\mathcal{A}_\sigma \simeq \frac{1}{2} \int d\zeta d^3x \left[\sigma'^2 + \vec{\nabla}\sigma \cdot \vec{\nabla}\sigma + \frac{R''}{R} \sigma^2 \right]. \quad (8.8)$$

We now do a canonical quantization of the system by imposing the conformal time commutation relations

$$[\sigma(\zeta, \vec{x}), \pi(\zeta, \vec{x}')] = i\hbar \delta(\vec{x} - \vec{x}'), \quad (8.9)$$

$$[\sigma(\zeta, \vec{x}), \sigma(\zeta, \vec{x}')] = 0 = [\pi(\zeta, \vec{x}), \pi(\zeta, \vec{x}')], \quad (8.10)$$

where $\pi(\zeta, \vec{x}) = \sigma'$. A Fourier expansion of $\sigma(\zeta, \vec{x})$ leads to

$$\sigma(\zeta, \vec{x}) = \int \frac{d^3k}{(2\pi)^{3/2}} \left[a(\vec{k}) \sigma(\vec{k}, \zeta) e^{i\vec{k} \cdot \vec{x}} + a^\dagger(\vec{k}) \sigma^*(\vec{k}, \zeta) e^{-i\vec{k} \cdot \vec{x}} \right], \quad (8.11)$$

and quantization of the creation and the destruction operators $a(\vec{k})$ and $a(\vec{k})^\dagger$ so that

$$\begin{aligned} [a(\vec{k}), a^\dagger(\vec{k}')] &= \delta(\vec{k} - \vec{k}'), \\ [a(\vec{k}), a(\vec{k}')] &= 0 = [a^\dagger(\vec{k}), a^\dagger(\vec{k}')] \end{aligned} \quad (8.12)$$

where the Fourier component $\sigma(\vec{k}, \zeta)$ obey the equations of motion

$$\sigma''(\vec{k}, \zeta) + \left(k^2 - \frac{2}{\zeta^2}\right) \sigma(\vec{k}, \zeta) = 0. \quad (8.13)$$

In Eq.(8.13) we used $R''/R = 2/\zeta^2$. This result follows from the fact that for the case when $H = \dot{R}/R$ is a constant the scale factor and the conformal time are related so that $R(\zeta) = -(H\zeta)^{-1}$. A specific solution to Eq.(8.13) [58–60] is

$$\sigma(\zeta, \vec{k}) = \sqrt{\frac{\hbar}{2k}} \left(1 - \frac{i}{k\zeta} \right) e^{-ik\zeta}. \quad (8.14)$$

Using the commutation relations of Eq.(8.12) and the result above the correlation function $\langle 0 | \sigma(\vec{x}) \sigma(\vec{y}) | 0 \rangle$ is given by

$$\langle 0 | \sigma(\vec{x}) \sigma(\vec{y}) | 0 \rangle = \int d^3k e^{i\vec{k} \cdot (\vec{x} - \vec{y})} \frac{|\sigma(\zeta, \vec{k})|^2}{(2\pi)^3}. \quad (8.15)$$

The power spectrum for σ is given by

$$\mathcal{P}_\sigma(k) = \frac{k^3}{2\pi^2} |\sigma(\zeta, \vec{k})|^2. \quad (8.16)$$

The comoving curvature perturbation \mathcal{R} is defined by

$$\mathcal{R} = \frac{\mathcal{H}}{\phi'} \delta\phi - \gamma \quad (8.17)$$

Thus $\mathcal{R} = -\sigma/z$ and the power spectrum for the curvature perturbation $\mathcal{P}_\mathcal{R}(k)$ is given by

$$\mathcal{P}_\mathcal{R}(k) = \frac{k^3}{2\pi^2} z^{-2} |\sigma(\zeta, \vec{k})|^2. \quad (8.18)$$

Now for the case when the wavelength is larger than the Hubble radius one has $k|\zeta| \ll 1$. Further using the result $R(\zeta) = -(H\zeta)^{-1}$ and Eq.(8.14) in Eq.(8.18) and reverting to the cosmic time rather than using the conformal time one gets

$$\mathcal{P}_{\mathcal{R}} \simeq \frac{\hbar}{4\pi^2} \left(H^4 / \dot{\phi}^2 \right)_{k=RH} . \quad (8.19)$$

Computation of the tensor power spectrum is very similar to the scalar case except for the polarization and one gets

$$\mathcal{P}_t = \frac{2\hbar}{\pi^2} \left(\frac{H}{M_{Pl}} \right)_{k=RH}^2 . \quad (8.20)$$

$\mathcal{P}_{\mathcal{R}}$ and \mathcal{P}_t can be exhibited in terms of the inflaton potential. Here one finds

$$\begin{aligned} \mathcal{P}_{\mathcal{R}} &= \frac{1}{12\pi^2} \left(\frac{V^3}{M_{Pl}^6 V'^2} \right)_{k=RH} , \\ \mathcal{P}_t &= \frac{2}{3\pi^2} \left(\frac{V}{M_{Pl}^4} \right)_{k=RH} . \end{aligned} \quad (8.21)$$

Models of inflation are often parametrized in terms of the so called slow roll parameters ϵ, η defined by

$$\epsilon = \frac{1}{2} \left(\frac{M_{Pl} V'}{V} \right)^2 , \quad \eta = \left| \frac{M_{Pl}^2 V''(\phi)}{V(\phi)} \right| . \quad (8.22)$$

The spectral indices n_s and n_t (see Eqs.(5.1) and (5.2)) are related to them by

$$n_s = 1 - 6\epsilon + 2\eta, \quad n_t = -2\epsilon, \quad r = 16\epsilon. \quad (8.23)$$

where r is defined by Eq.(5.3). Eq.(8.23) is for the standard single-field inflation and gives the prediction $n_t = -r/8$. Small deviations from this result can occur for the effective single-field case and the size of the deviations will depend on the specifics of the inputs. A more detailed discussion of this is given in section 5.2.

9 Appendix C: Emergence of a flat inflation potential for axions

Here we give an illustration of how a flat inflation potential for axions arises from a superposition of cosine functions with the specific case of Fig.(7) in mind. To exhibit this we begin by simplifying Eq.(4.13) for the case of Fig.(7), i.e., $q = 3$, and $\gamma_k = k$ for $k = 1, 2, 3$. Setting $M_{Pl} = 1$, we get:

$$\begin{aligned}
V_3(b) = & -\frac{1}{f^2}(4e^{2f^2+2}(-2A_1^2(4f^4+f^2+1) - eA_1(A_2(4f^2+3)f^2 + 2eA_3(4f^4+5f^2+3)) \\
& + e^3A_2A_3(4f^4+7f^2+12))) \left(1 - \cos\left(\frac{b}{\sqrt{2}f}\right)\right) \\
& + \frac{1}{f^2}(2e^{2f^2+2}(A_1^2(-(4f^4+f^2)) + 2eA_1(A_2(8f^4+6f^2+4) - eA_3(4f^4+5f^2+6)) \\
& + 4e^2A_2(A_2(4f^4+5f^2+4) + eA_3(4f^4+7f^2+6)))) \left(1 - \cos\left(\frac{2b}{\sqrt{2}f}\right)\right) \\
& + \frac{1}{f^2}(4e^{2f^2+3}(A_1(2eA_3(4f^4+5f^2+3) - A_2f^2(4f^2+3)) \\
& + 2e^2A_3(A_2(4f^4+7f^2+6) + eA_3(4f^4+9f^2+9)))) \left(1 - \cos\left(\frac{3b}{\sqrt{2}f}\right)\right) \\
& - 2(A_2^2 + 2A_1A_3)e^{2f^2+4}(4f^2+5) \left(1 - \cos\left(\frac{4b}{\sqrt{2}f}\right)\right) \\
& - 4A_2A_3e^{2f^2+5}(4f^2+7) \left(1 - \cos\left(\frac{5b}{\sqrt{2}f}\right)\right) \\
& - 2A_3^2e^{2f^2+6}(4f^2+9) \left(1 - \cos\left(\frac{6b}{\sqrt{2}f}\right)\right). \tag{9.1}
\end{aligned}$$

Substituting $f = 0.8211$, $A_2/A_1 = 8.9588 \times 10^{-2}$, $A_3/A_1 = 4.1713 \times 10^{-3}$, as in Fig.(7), we obtain:

$$\begin{aligned}
V_3(b)/A_1^2 = & 1398.96 \left(1 - \cos\left(\frac{b}{\sqrt{2}f}\right)\right) + 427.466 \left(1 - \cos\left(\frac{2b}{\sqrt{2}f}\right)\right) \\
& - 35.4939 \left(1 - \cos\left(\frac{3b}{\sqrt{2}f}\right)\right) - 52.9837 \left(1 - \cos\left(\frac{4b}{\sqrt{2}f}\right)\right) \\
& - 8.28504 \left(1 - \cos\left(\frac{5b}{\sqrt{2}f}\right)\right) - 0.632442 \left(1 - \cos\left(\frac{6b}{\sqrt{2}f}\right)\right). \tag{9.2}
\end{aligned}$$

Eq.(9.2) is the potential used in the analysis of Fig. (7).

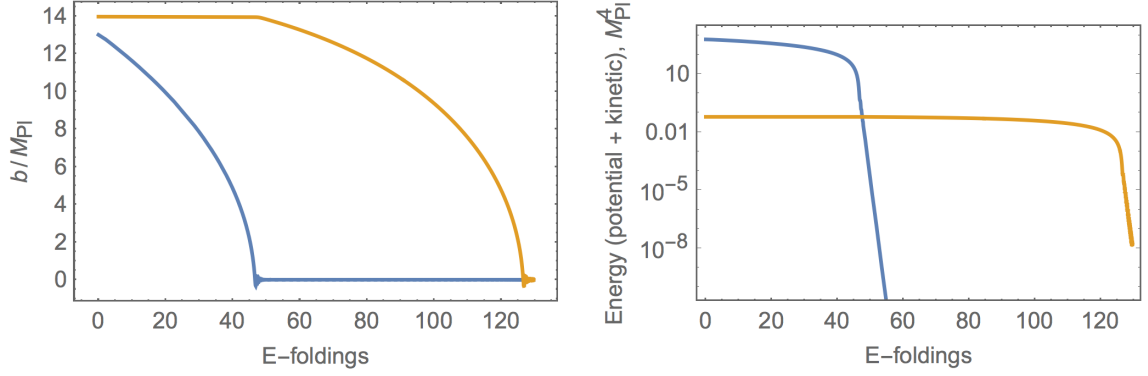


Figure 1. Left panel: fast and slow field components as a function of the e-foldings. Right panel: energy of the slow and fast field components as a function of e-foldings. Slow field energy is defined as $E_{\text{slow}} = V_{\text{slow}}(b_-) + \frac{1}{2}\dot{b}_-^2$. Fast field energy is defined as $E_{\text{fast}} = V_{\text{full}}(b_-, b_+) - V_{\text{slow}}(b_-) + \frac{1}{2}\dot{b}_+^2$. One can see that the fast component starts larger, but then the slow component overtakes it. Here $B = 10^{-4}$.

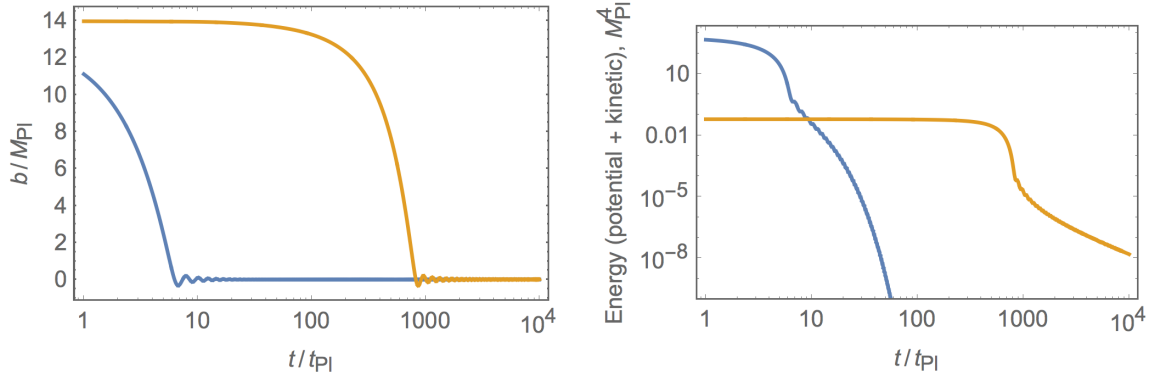


Figure 2. Left panel: fast and slow field components as a function of time. Right panel: energy of the slow and fast field components as a function of time. Slow field energy is defined as $E_{\text{slow}} = V_{\text{slow}}(b_-) + \frac{1}{2}\dot{b}_-^2$. Fast field energy is defined as $E_{\text{fast}} = V_{\text{full}}(b_-, b_+) - V_{\text{slow}}(b_-) + \frac{1}{2}\dot{b}_+^2$. One can see that the fast component starts larger, but then the slow component overtakes it. Note the logarithmic scale of time. Here $B = 10^{-4}$.

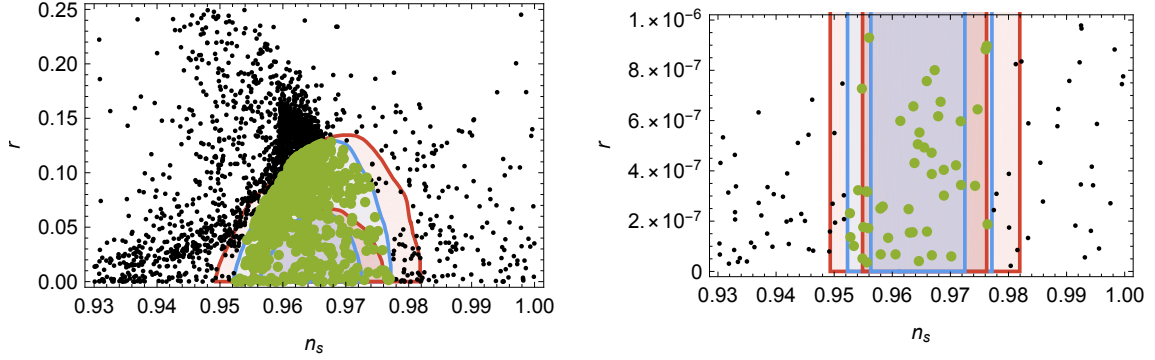


Figure 3. Monte-Carlo analysis for the model with $G_4 = 1$, $G_5 \neq 0$ for the entire input parameters space shown in observables space. The blue region corresponds to 68% (inner contour) and 95% CL (outer contour) regions of Planck experiment [11] TT, TE, EE + lowP (include polarization data). The red regions correspond to Planck TT+lowP (do not include polarization data). For a discussion of TT, TE, EE + lowP see reference [11]. The green and the black scatter points corresponds to scenarios where b_- reaches global minimum at the end of inflation, and the green scatter points satisfy experimental bounds on n_s and r for the TT, TE, EE + lowP Planck data analysis. All model points have $N = [50, 60]$. The decay constant $f < M_{Pl}$ for all points on the right panel.

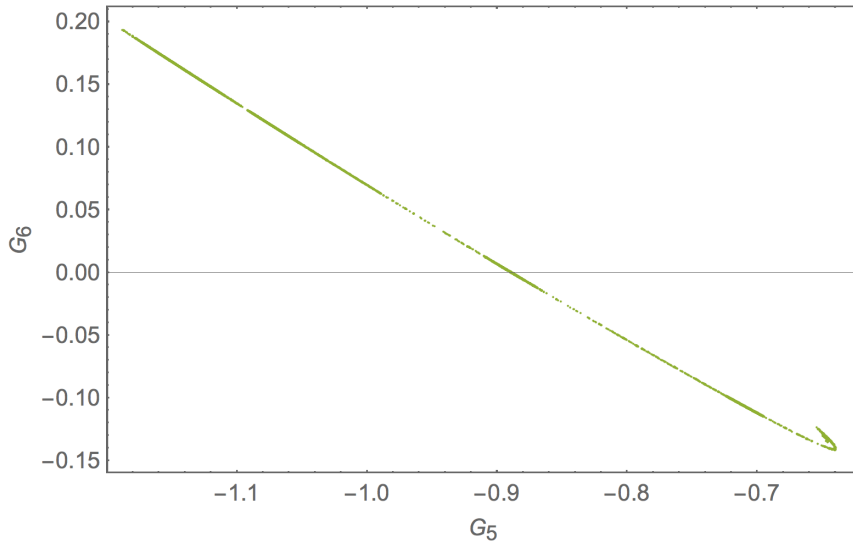


Figure 4. Exhibition of a region in $|G_6| < |G_5|$ plane where all experimental constraints are satisfied. The region exhibited does not exclude other regions where consistent inflation can occur. The analysis shows that inflation can occur in extended regions of the parameter space of models.

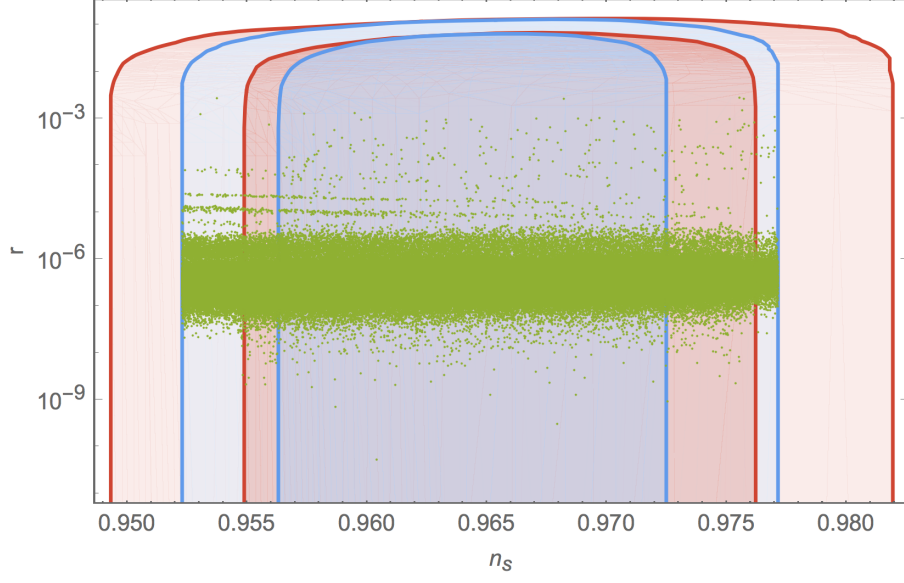


Figure 5. Monte-Carlo analysis when $G_4 = 1$, $G_5 \neq 0$, $G_6 \neq 0$ for the entire input parameters space shown in (n_s, r) space. The entire set of points shown pass all experimental tests. Note the log scale on the r axis.

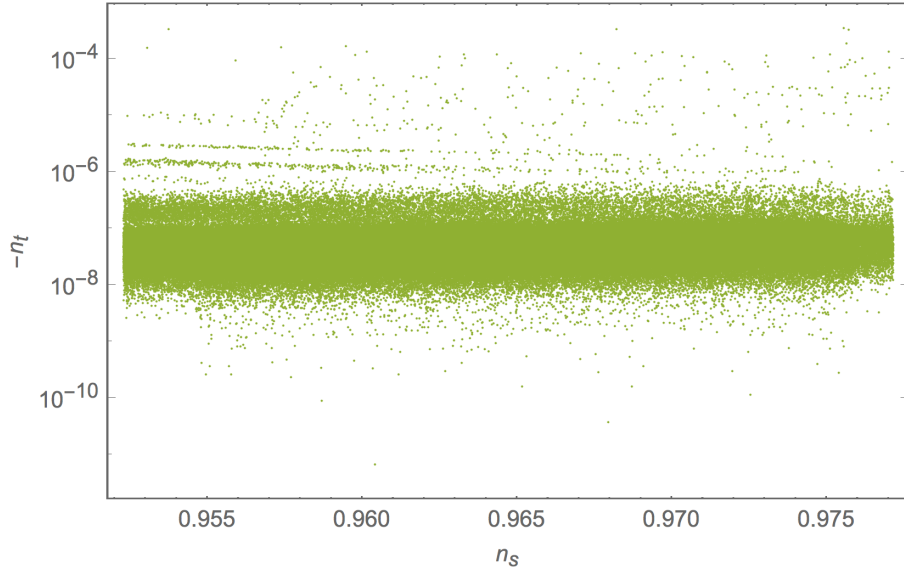


Figure 6. Monte-Carlo analysis when $G_4 = 1$, $G_5 \neq 0$, $G_6 \neq 0$ for the entire input parameters space shown in (n_s, n_t) space for the same dataset as in Fig.(5). Note the log scale on the $-n_t$ axis.

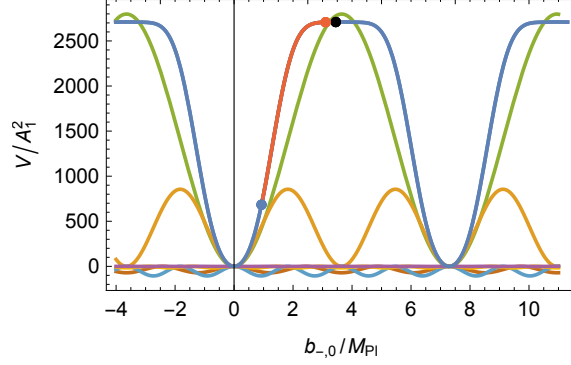


Figure 7. The red and blue curve shows a generic example of a slow-roll potential in $q = 3$ supergravity model. Here $A_2/A_1 = 8.9588 \times 10^{-2}$, $A_3/A_1 = 4.1713 \times 10^{-3}$, $\gamma_k = k$, $f/M_{Pl} = 0.8211$, $b_{-,0}/M_{Pl} = 3.448$, $N_{\text{pivot}} = 56.6$. For this case, the observables are $n_s = 0.9714$, $n_t = -1.34 \times 10^{-5}$, $r = 1.07 \times 10^{-4}$. The black dot corresponds to the initial value of the field, the red dot to horizon exit, and the blue dot to the end of inflation. Other curves show contributions to the potential from individual cosine modes. Thus the green curve is plot of the first term in Eq.(9.2) in Appendix Sec.(9) while the brown curve is plot of the second term in Eq.(9.2). The remaining terms in Eq.(9.2) are curves with small amplitudes in the plot.

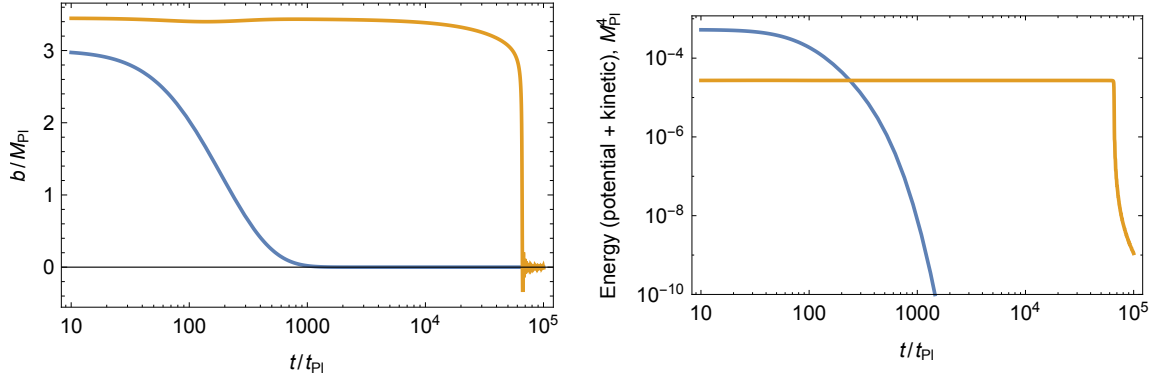


Figure 8. Fast vs. slow field evolution for the case of Fig.(7). Left panel: fast and slow field components as a function of time. Right panel: energy of the slow and fast field components as a function of time. Slow field energy is defined as $E_{\text{slow}} = V_{\text{slow}}(b_-) + \frac{1}{2}\dot{b}_-^2$. Fast field energy is defined as $E_{\text{fast}} = V_{\text{full}}(b_+, b_-) - V_{\text{slow}}(b_-) + \frac{1}{2}\dot{b}_+^2$. One can see that the fast component starts larger, but then the slow component overtakes it. Note the logarithmic scale of time. Here $A_1 = 10^{-4}M_{Pl}^2$.

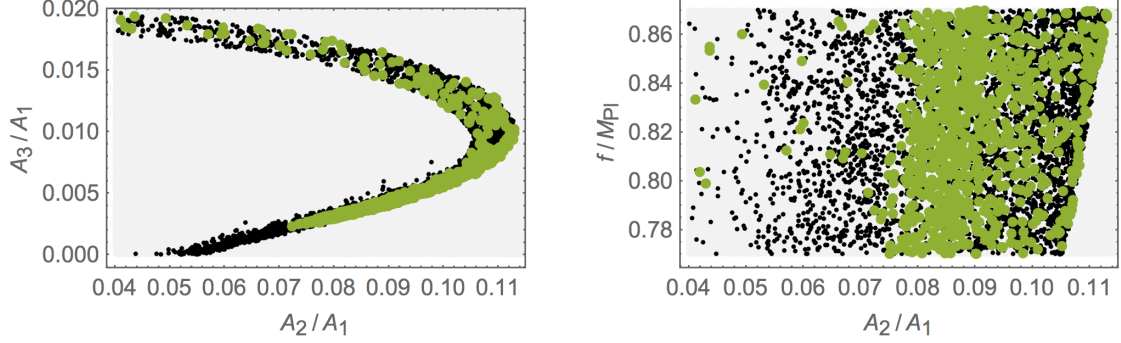


Figure 9. Left panel: A_3/A_1 vs. A_2/A_1 for the experimentally acceptable points for the $q = 3$ supergravity model in the input parameters space for the case of one pair of axions. Right panel: The same parameter space plotted in the f/M_{Pl} vs A_2/A_1 . The green and black parameter points have the same meaning as in Fig.(3). Note the entire parameter space of this supergravity model exhibited here has $f < M_{Pl}$.

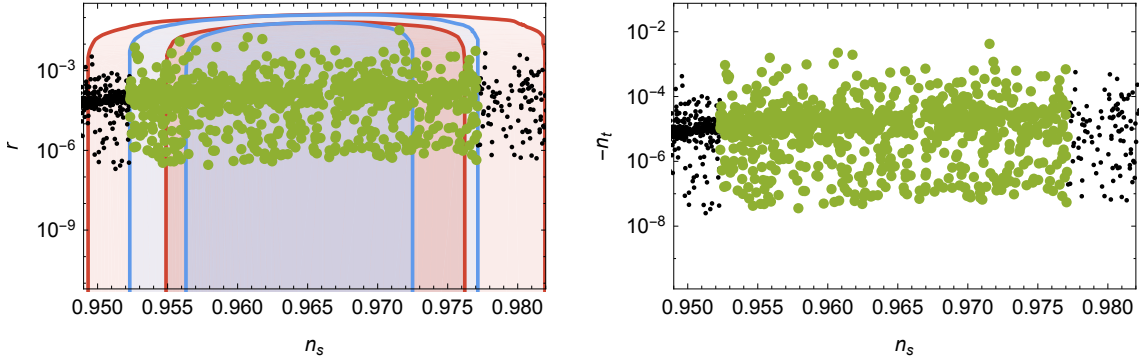


Figure 10. Left panel: Display of r vs n_s for the same parameter space as in Fig.(9). Right panel: Display n_t vs n_s for the same parameter space as in Fig.(9). The green and black parameter points have the same meaning as in Fig.(3).

References

- [1] A. H. Guth, Phys. Rev. D **23**, 347 (1981). doi:10.1103/PhysRevD.23.347
- [2] A. A. Starobinsky, Phys. Lett. **91B**, 99 (1980). doi:10.1016/0370-2693(80)90670-X
- [3] A. D. Linde, Phys. Lett. **108B**, 389 (1982). doi:10.1016/0370-2693(82)91219-9
- [4] A. Albrecht and P. J. Steinhardt, Phys. Rev. Lett. **48**, 1220 (1982). doi:10.1103/PhysRevLett.48.1220
- [5] K. Sato, Monthly Notices of the Royal Astronomical Society, Volume 195, Issue 3, 1 July 1981, Pages 467-479, <https://doi.org/10.1093/mnras/195.3.467>
- [6] A. D. Linde, Phys. Lett. **129B**, 177 (1983). doi:10.1016/0370-2693(83)90837-7
- [7] A. D. Linde, “Particle physics and inflationary cosmology,” Contemp. Concepts Phys. **5**, 1 (1990) [hep-th/0503203].
- [8] C. Cheung, P. Creminelli, A. L. Fitzpatrick, J. Kaplan and L. Senatore, JHEP **0803**, 014 (2008) doi:10.1088/1126-6708/2008/03/014 [arXiv:0709.0293 [hep-th]].
- [9] V. F. Mukhanov and G. V. Chibisov, Pis’ma Zh. Eksp. Teor. Fiz. **33**, 549 (1981) [JETP Lett. **33**, 532 (1981)]; S. W. Hawking, Phys. Lett. B **115**, 295 (1982); A. A. Starobinsky, Phys. Lett. B **117**, 175 (1982); A. H. Guth and S. Y. Pi, Phys. Rev. Lett. **49**, 1110 (1982); J. M. Bardeen, P. J. Steinhardt, and M. S. Turner, Phys. Rev. D **28**, 679 (1983).
- [10] R. Adam *et al.* [Planck Collaboration], Astron. Astrophys. **594**, A1 (2016) doi:10.1051/0004-6361/201527101 [arXiv:1502.01582 [astro-ph.CO]].
- [11] P. A. R. Ade *et al.* [Planck Collaboration], Astron. Astrophys. **594**, A20 (2016) doi:10.1051/0004-6361/201525898 [arXiv:1502.02114 [astro-ph.CO]].
- [12] P. A. R. Ade *et al.* [BICEP2 and Keck Array Collaborations], Phys. Rev. Lett. **116**, 031302 (2016) doi:10.1103/PhysRevLett.116.031302 [arXiv:1510.09217 [astro-ph.CO]].
- [13] K. Freese, J. A. Frieman and A. V. Olinto, Phys. Rev. Lett. **65**, 3233 (1990). doi:10.1103/PhysRevLett.65.3233
- [14] F. C. Adams, J. R. Bond, K. Freese, J. A. Frieman and A. V. Olinto, Phys. Rev. D **47**, 426 (1993) doi:10.1103/PhysRevD.47.426 [hep-ph/9207245].
- [15] T. Banks, M. Dine, P. J. Fox and E. Gorbatov, JCAP **0306**, 001 (2003) doi:10.1088/1475-7516/2003/06/001 [hep-th/0303252].
- [16] P. Svrcek and E. Witten, JHEP **0606**, 051 (2006) doi:10.1088/1126-6708/2006/06/051 [hep-th/0605206].
- [17] J. E. Kim, H. P. Nilles and M. Peloso, JCAP **0501**, 005 (2005) doi:10.1088/1475-7516/2005/01/005 [hep-ph/0409138].
- [18] C. Long, L. McAllister and P. McGuirk, Phys. Rev. D **90**, 023501 (2014) doi:10.1103/PhysRevD.90.023501 [arXiv:1404.7852 [hep-th]].
- [19] M. Berg, E. Pajer and S. Sjors, Phys. Rev. D **81**, 103535 (2010) doi:10.1103/PhysRevD.81.103535 [arXiv:0912.1341 [hep-th]].
- [20] S. Dimopoulos, S. Kachru, J. McGreevy and J. G. Wacker, JCAP **0808**, 003 (2008) doi:10.1088/1475-7516/2008/08/003 [hep-th/0507205].

- [21] R. Easther and L. McAllister, JCAP **0605**, 018 (2006) doi:10.1088/1475-7516/2006/05/018 [hep-th/0512102].
- [22] T. W. Grimm, Phys. Rev. D **77**, 126007 (2008) doi:10.1103/PhysRevD.77.126007 [arXiv:0710.3883 [hep-th]].
- [23] R. Kallosh, N. Sivanandam and M. Soroush, Phys. Rev. D **77**, 043501 (2008) doi:10.1103/PhysRevD.77.043501 [arXiv:0710.3429 [hep-th]].
- [24] M. E. Olsson, JCAP **0704**, 019 (2007) doi:10.1088/1475-7516/2007/04/019 [hep-th/0702109].
- [25] D. Battfeld and T. Battfeld, JCAP **0705**, 012 (2007) doi:10.1088/1475-7516/2007/05/012 [hep-th/0703012].
- [26] S. A. Kim, A. R. Liddle and D. Seery, Phys. Rev. D **85**, 023532 (2012) doi:10.1103/PhysRevD.85.023532 [arXiv:1108.2944 [astro-ph.CO]].
- [27] S. A. Kim, A. R. Liddle and D. Seery, Phys. Rev. Lett. **105**, 181302 (2010) doi:10.1103/PhysRevLett.105.181302 [arXiv:1005.4410 [astro-ph.CO]].
- [28] T. Rudelius, JCAP **1504**, no. 04, 049 (2015) doi:10.1088/1475-7516/2015/04/049 [arXiv:1409.5793 [hep-th]].
- [29] N. Arkani-Hamed, H. C. Cheng, P. Creminelli and L. Randall, JCAP **0307**, 003 (2003) doi:10.1088/1475-7516/2003/07/003 [hep-th/0302034].
- [30] D. E. Kaplan and N. J. Weiner, JCAP **0402**, 005 (2004) doi:10.1088/1475-7516/2004/02/005 [hep-ph/0302014].
- [31] D. Green, B. Horn, L. Senatore and E. Silverstein, Phys. Rev. D **80**, 063533 (2009) doi:10.1103/PhysRevD.80.063533 [arXiv:0902.1006 [hep-th]].
- [32] A. Arvanitaki, S. Dimopoulos, S. Dubovsky, N. Kaloper and J. March-Russell, Phys. Rev. D **81**, 123530 (2010) doi:10.1103/PhysRevD.81.123530 [arXiv:0905.4720 [hep-th]].
- [33] E. Pajer and M. Peloso, Class. Quant. Grav. **30**, 214002 (2013) doi:10.1088/0264-9381/30/21/214002 [arXiv:1305.3557 [hep-th]].
- [34] D. J. E. Marsh, Phys. Rept. **643**, 1 (2016) doi:10.1016/j.physrep.2016.06.005 [arXiv:1510.07633 [astro-ph.CO]].
- [35] P. Nath, “Supersymmetry, Supergravity, and Unification,” Cambridge, Uk: Univ. Pr. (2016) 520 P. (Cambridge Monographs On Mathematical Physics).
- [36] J. R. Ellis, D. V. Nanopoulos, K. A. Olive and K. Tamvakis, Nucl. Phys. B **221**, 524 (1983). doi:10.1016/0550-3213(83)90592-8
- [37] H. Murayama, H. Suzuki, T. Yanagida and J. Yokoyama, Phys. Rev. D **50**, 2356 (1994); E. J. Copeland, A. R. Liddle, D. H. Lyth, E. D. Stewart and D. Wands, Phys. Rev. D **49**, 6410 (1994); E. D. Stewart, Phys. Rev. D **51**, 6847 (1995); G. R. Dvali, Q. Shafi and R. K. Schaefer, Phys. Rev. Lett. **73**, 1886 (1994) doi:10.1103/PhysRevLett.73.1886 [hep-ph/9406319]; P. Binetruy and G. R. Dvali, Phys. Lett. B **388**, 241 (1996);
- [38] B. Kors and P. Nath, Nucl. Phys. B **711**, 112 (2005). [hep-th/0411201].
- [39] M. Yamaguchi, Class. Quant. Grav. **28**, 103001 (2011); M. Kawasaki, M. Yamaguchi and T. Yanagida, Phys. Rev. Lett. **85**, 3572 (2000); M. Yamaguchi and J. 'i. Yokoyama, Phys. Rev. D **63**, 043506 (2001) [hep-ph/0007021]; D. Baumann and D. Green, “Signatures of Supersymmetry from the Early Universe,” Phys. Rev. D **85** (2012) 103520 [arXiv:1109.0292]

- [hep-th]]. M. Yamaguchi, Phys. Rev. D **64**, 063502 (2001) [hep-ph/0103045]; M. Kawasaki and M. Yamaguchi, Phys. Rev. D **65**, 103518 (2002) [hep-ph/0112093]; M. Yamaguchi and J. 'i. Yokoyama, Phys. Rev. D **68**, 123520 (2003) [hep-ph/0307373]; P. Brax and J. Martin, Phys. Rev. D **72**, 023518 (2005) [hep-th/0504168]; R. Kallosh, Lect. Notes Phys. **738**, 119 (2008) [hep-th/0702059 [HEP-TH]]; S. C. Davis and M. Postma, JCAP **0803**, 015 (2008) [arXiv:0801.4696 [hep-ph]]; F. Takahashi, Phys. Lett. B **693**, 140 (2010) [arXiv:1006.2801 [hep-ph]]; K. Nakayama and F. Takahashi, JCAP **1011**, 009 (2010) [arXiv:1008.2956 [hep-ph]]; R. Kallosh and A. Linde, JCAP **1011**, 011 (2010) [arXiv:1008.3375 [hep-th]]; M. Kawasaki, N. Kitajima and K. Nakayama, Phys. Rev. D **83**, 123521 (2011) [arXiv:1104.1262 [hep-ph]]; J. Ellis, D. V. Nanopoulos and K. A. Olive, Phys. Rev. Lett. **111**, 111301 (2013) Erratum: [Phys. Rev. Lett. **111**, no. 12, 129902 (2013)] doi:10.1103/PhysRevLett.111.129902, 10.1103/PhysRevLett.111.111301 [JarXiv:1305.1247 [hep-th]]; M. Czerny, T. Higaki and F. Takahashi, JHEP **1405**, 144 (2014) doi:10.1007/JHEP05(2014)144 [arXiv:1403.0410 [hep-ph]]; T. Kobayashi, S. Uemura and J. Yamamoto, Phys. Rev. D **96**, no. 2, 026007 (2017) doi:10.1103/PhysRevD.96.026007 [arXiv:1705.04088 [hep-ph]]; N. Okada and Q. Shafi, arXiv:1709.04610 [hep-ph].
- [40] J. J. Blanco-Pillado, C. P. Burgess, J. M. Cline, C. Escoda, M. Gomez-Reino, R. Kallosh, A. D. Linde and F. Quevedo, JHEP **0411**, 063 (2004) doi:10.1088/1126-6708/2004/11/063 [hep-th/0406230].
- [41] S. Krippendorff and F. Quevedo, JHEP **0911**, 039 (2009) doi:10.1088/1126-6708/2009/11/039 [arXiv:0901.0683 [hep-th]].
- [42] M. Cicoli, K. Dutta, A. Maharana and F. Quevedo, JCAP **1608**, no. 08, 006 (2016) doi:10.1088/1475-7516/2016/08/006 [arXiv:1604.08512 [hep-th]].
- [43] R. D. Peccei and H. R. Quinn, Phys. Rev. D **16**, 1791 (1977). doi:10.1103/PhysRevD.16.1791
- [44] S. Weinberg, Phys. Rev. Lett. **40**, 223 (1978). doi:10.1103/PhysRevLett.40.223
- [45] F. Wilczek, Phys. Rev. Lett. **40**, 279 (1978). doi:10.1103/PhysRevLett.40.279
- [46] J. Halverson, C. Long and P. Nath, Phys. Rev. D **96**, no. 5, 056025 (2017) doi:10.1103/PhysRevD.96.056025 [arXiv:1703.07779 [hep-ph]].
- [47] M. Cvetič, J. Halverson and R. Richter, JHEP **1007**, 005 (2010) doi:10.1007/JHEP07(2010)005 [arXiv:0909.4292 [hep-th]].
- [48] Y. Nambu and G. Jona-Lasinio, Phys. Rev. **122**, 345 (1961); J. Goldstone, Nuovo Cim. **19**, 154 (1961); J. Goldstone, A. Salam and S. Weinberg, Phys. Rev. **127**, 965 (1962).
- [49] A. H. Chamseddine, R. L. Arnowitt and P. Nath, Phys. Rev. Lett. **49**, 970 (1982). doi:10.1103/PhysRevLett.49.970
- [50] E. Cremmer, S. Ferrara, L. Girardello and A. Van Proeyen, Nucl. Phys. B **212**, 413 (1983). doi:10.1016/0550-3213(83)90679-X
- [51] P. Nath, R. L. Arnowitt and A. H. Chamseddine, Nucl. Phys. B **227**, 121 (1983). doi:10.1016/0550-3213(83)90145-1
- [52] S. M. Leach, A. R. Liddle, J. Martin and D. J. Schwarz, Phys. Rev. D **66**, 023515 (2002) doi:10.1103/PhysRevD.66.023515 [astro-ph/0202094].
- [53] M. Dias, J. Frazer and D. Seery, JCAP **1512**, no. 12, 030 (2015) doi:10.1088/1475-7516/2015/12/030 [arXiv:1502.03125 [astro-ph.CO]].

- [54] D. H. Lyth and A. Riotto, Phys. Rept. **314**, 1 (1999) doi:10.1016/S0370-1573(98)00128-8 [hep-ph/9807278].
- [55] A. R. Liddle and D. H. Lyth, Cambridge, UK: Univ. Pr. (2000) 400 p
- [56] D. Langlois, Lect. Notes Phys. **800**, 1 (2010) [arXiv:1001.5259 [astro-ph.CO]].
- [57] D. Baumann, arXiv:0907.5424 [hep-th].
- [58] T. S. Bunch and P. C. W. Davies, Proc. Roy. Soc. Lond. A **360**, 117 (1978). doi:10.1098/rspa.1978.0060
- [59] N. A. Chernikov and E. A. Tagirov, Ann. Inst. H. Poincare Phys. Theor. A **9**, 109 (1968).
- [60] C. Schomblond and P. Spindel, Ann. Inst. H. Poincare Phys. Theor. **25**, 67 (1976).
- [61] R. L. Arnowitt and P. Nath, Phys. Rev. Lett. **69**, 725 (1992). doi:10.1103/PhysRevLett.69.725
- [62] D. H. Lyth, Phys. Rev. Lett. **78**, 1861 (1997) doi:10.1103/PhysRevLett.78.1861 [hep-ph/9606387].
- [63] M. A. Amin, M. P. Hertzberg, D. I. Kaiser and J. Karouby, Int. J. Mod. Phys. D **24**, 1530003 (2014) doi:10.1142/S0218271815300037 [arXiv:1410.3808 [hep-ph]].
- [64] S. Kachru, R. Kallosh, A. D. Linde and S. P. Trivedi, Phys. Rev. D **68**, 046005 (2003).
- [65] V. Balasubramanian, P. Berglund, J. P. Conlon and F. Quevedo, JHEP **0503**, 007 (2005).
- [66] J. J. Blanco-Pillado, C. P. Burgess, J. M. Cline, C. Escoda, M. Gomez-Reino, R. Kallosh, A. D. Linde and F. Quevedo, “Racetrack inflation,” JHEP **0411**, 063 (2004) doi:10.1088/1126-6708/2004/11/063 [hep-th/0406230].
- [67] Z. Lalak, G. G. Ross and S. Sarkar, “Racetrack inflation and assisted moduli stabilisation,” Nucl. Phys. B **766**, 1 (2007) doi:10.1016/j.nuclphysb.2006.06.041 [hep-th/0503178].
- [68] B. Greene and A. Weltman, “An Effect of alpha’ corrections on **racetrack inflation**,” JHEP **0603**, 035 (2006) doi:10.1088/1126-6708/2006/03/035 [hep-th/0512135].
- [69] J. J. Blanco-Pillado, C. P. Burgess, J. M. Cline, C. Escoda, M. Gomez-Reino, R. Kallosh, A. D. Linde and F. Quevedo, “Inflating in a better racetrack,” JHEP **0609**, 002 (2006) doi:10.1088/1126-6708/2006/09/002 [hep-th/0603129].
- [70] C. Y. Sun and D. H. Zhang, “The Non-Gaussianity of Racetrack Inflation Models,” Commun. Theor. Phys. **48**, 189 (2007) doi:10.1088/0253-6102/48/1/038 [astro-ph/0604298].
- [71] P. Brax, A. C. Davis, S. C. Davis, R. Jeannerot and M. Postma, “D-term Uplifted Racetrack Inflation,” JCAP **0801**, 008 (2008) doi:10.1088/1475-7516/2008/01/008 [arXiv:0710.4876 [hep-th]].
- [72] W. Y. Wen, ‘Inflation in a refined racetrack,’ arXiv:0712.0458 [hep-th].
- [73] P. Brax, S. C. Davis and M. Postma, “The Robustness of $n(s) < 0.95$ in racetrack inflation,” JCAP **0802**, 020 (2008) doi:10.1088/1475-7516/2008/02/020 [arXiv:0712.0535 [hep-th]].
- [74] W. Y. Wen, “Effects of open string moduli on racetrack inflation,” Mod. Phys. Lett. A **23**, 1589 (2008). doi:10.1142/S0217732308027989
- [75] P. Brax, C. van de Bruck, A. C. Davis, S. C. Davis, R. Jeannerot and M. Postma, “Racetrack Inflation and Cosmic Strings,” JCAP **0807**, 018 (2008) doi:10.1088/1475-7516/2008/07/018 [arXiv:0805.1171 [hep-th]].

- [76] H. Y. Chen, L. Y. Hung and G. Shiu, “Inflation on an Open Racetrack,” JHEP **0903**, 083 (2009) doi:10.1088/1126-6708/2009/03/083 [arXiv:0901.0267 [hep-th]].
- [77] M. Badziak and M. Olechowski, “Inflation with racetrack superpotential and matter field,” JCAP **1002**, 026 (2010) doi:10.1088/1475-7516/2010/02/026 [arXiv:0911.1213 [hep-th]].
- [78] R. Allahverdi, B. Dutta and K. Sinha, “Low-scale Inflation and Supersymmetry Breaking in Racetrack Models,” Phys. Rev. D **81**, 083538 (2010) doi:10.1103/PhysRevD.81.083538 [arXiv:0912.2324 [hep-th]].
- [79] M. Olechowski, “Inflation with racetrack superpotential and matter field,” J. Phys. Conf. Ser. **259**, 012028 (2010). doi:10.1088/1742-6596/259/1/012028
- [80] M. Badziak, “F-term uplifted racetrack inflation,” arXiv:1005.5537 [hep-th].
- [81] T. Higaki and F. Takahashi, JHEP **1407**, 074 (2014) doi:10.1007/JHEP07(2014)074 [arXiv:1404.6923 [hep-th]].
- [82] T. Higaki and F. Takahashi, Phys. Lett. B **744**, 153 (2015) doi:10.1016/j.physletb.2015.03.052 [arXiv:1409.8409 [hep-ph]].
- [83] K. Kadota, T. Kobayashi, A. Oikawa, N. Omoto, H. Otsuka and T. H. Tatsuishi, JCAP **1610**, no. 10, 013 (2016) doi:10.1088/1475-7516/2016/10/013 [arXiv:1606.03219 [hep-ph]].
- [84] T. Kobayashi, A. Oikawa, N. Omoto, H. Otsuka and I. Saga, Phys. Rev. D **95**, no. 6, 063514 (2017) doi:10.1103/PhysRevD.95.063514 [arXiv:1609.05624 [hep-ph]].
- [85] A. Ernst, A. Ringwald and C. Tamarit, arXiv:1801.04906 [hep-ph].